^{85}Rb D1-line CPT Atomic Clock With Low Power Consumption

Shigeyoshi Goka
Electrical & Electronic Engineering
Tokyo Metropolitan University
Tokyo, Japan
goka@tmu.ac.jp

Abstract— **This paper describes the investigation of a ^{85}Rb D1-line coherent population trapping (CPT) atomic clock with a Rb gas-cell containing a natural mixture of Rb atoms and buffer gas. The choice of ^{85}Rb rather than conventional ^{87}Rb is dictated by the lower ground-state hyperfine-splitting frequency, which leads to less than one-half the required RF power and more effective RF-related circuit designs. In this paper, the modulation profiles, the CPT resonances, and the long-term frequency stabilities of the CPT resonance for ^{85}Rb D1 and D2 lines are presented. The frequency deviations for D1 and D2 lines are measured using a same experimental setup except for VCSEL wavelength and RF power. The Allan deviations, estimated from the frequency deviations, are < 2.5x10^{-12}/day for D1 line and < 4.0x10^{-12}/day for D2 line. In the case of D1 excitation, required RF frequency is 1.5 GHz and its power is only -8.0 dBm.**

I. INTRODUCTION

Relatively compact and inexpensive atomic frequency references are available commercially. An alkali-vapor cell and an external microwave cavity are used in these references to sense the transitions between ground and excited states [1]. The cavity size is determined by the transition wavelength of the alkali atoms. In addition, keeping cavity and gas cell temperature constant requires a several Watts of power because of the large cavity volume. As far as using a cavity, there are limitations of miniaturization and low power consumption. Compact frequency references with Low-cost, low-power consumption, and good long-term stability (~10^{-11} /day) have been in demand for portable equipment such as global-positioning system receivers, in-field telecommunication devices, and various kinds of measuring instruments [2,3]. As atomic clocks based on coherent population trapping (CPT) meets this demand, CPT based atomic clocks with a vertical-cavity surface-emitting laser (VCSEL) have been extensively progressed [3-13]. Since the most advantageous feature of a CPT resonance is that it does not require a large microwave cavity [14,15], a selection of alkali-atoms is not limited by its transition frequency. For such CPT-based atomic clocks, ^{87}Rb and Cs vapors are typically used and their required source radio frequency (RF) is 3.4 and 4.6 GHz, respectively. In electrical circuits, energy loss in an internal parasitic capacitance increases proportional to RF frequency because voltage changing of a RF signal requires extra current to charge and discharge the parasitic capacitance in every period of the RF signal [16]. In the microwave frequency range, the energy loss of the parasitic capacitance occupies power dissipation of a RF circuit. For the example, a miniaturized CPT-based atomic clock [17] has an RF oscillator and related PLL circuit power consumption of 57 mW, which is more than half the total power (108 mW) in spite of required RF output power is nearly 0 dBm (1 mW). Therefore, reducing the RF frequency can effectively reduce total power required.

An ^{85}Rb vapor-cell CPT atomic clock is developed for low-power operation. The choice of ^{85}Rb rather than conventional ^{87}Rb was dictated by the lower ground-state hyperfine-splitting frequency [18], which leads to less than one-half of the required power of the laser modulation sources and more effective RF circuit designs. In the previous work [19-20], I reported that the good long-term frequency stabilities of the ^{85}Rb D2-line CPT atomic clock, and that the feasibility of switching between low-power (^{85}Rb) and high-stability (^{87}Rb) operation modes by simply changing the RF frequency were reported. Since D1 excitation can generate a larger contrast of CPT resonance than that of D2 excitation in ^{85}Rb vapor [21], it is necessary to investigate an ^{85}Rb D1-line CPT atomic clock for low power consumption.

This paper describes the investigation of an ^{85}Rb D1-line CPT atomic clock with a Rb gas-cell containing a natural mixture of Rb atoms and N_2 buffer gas. The frequency deviations for D1 and D2 lines are measured using a same experimental setup except for VCSEL wavelength and RF power. The Allan deviations are also estimated from the frequency deviations.

978-1-4244-3510-4/09/$25.00 ©2009 IEEE

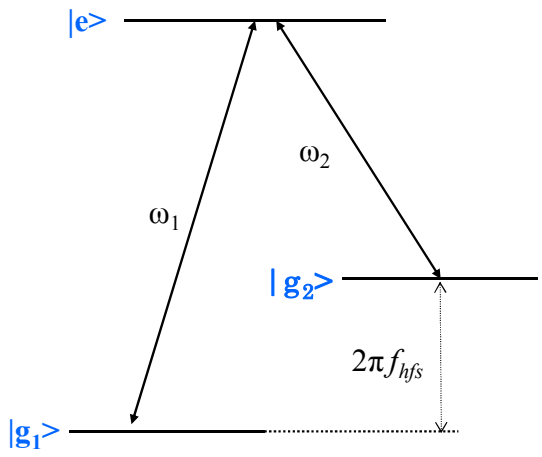

Figure 1. Three level Λ system in alkali-metal atoms

TABLE I. WAVELENGTH OF LIGHT FIELD FOR D_1 AND D_2 LINES AND GROUND-STATE HYPERFINE-SPLITTING FREQUENCY

Alkali atom	D1 line [nm]	D2 line [nm]	f_{hfs} [GHz]	$f_{hfs}/2$ [GHz]
Cs	894	852	9.2	4.6
^{87}Rb	795	780	6.8	3.4
^{85}Rb			3.0	1.5

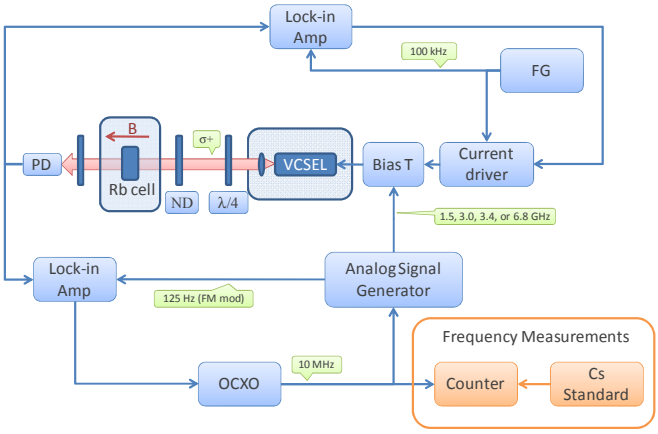

Figure 2. Schematic of measurement system

II. THREE-LEVEL Λ SYSTEM IN ALKALI ATOMS

Figure 1 shows so-called Λ systems with two long-lived ground states $|g_1\rangle$ and $|g_2\rangle$ and one excited state $|e\rangle$. The wavelength of the light field between $|g_n\rangle$ and $|e\rangle$ for D1 and D2 lines, and the ground-state hyperfine-splitting frequency f_{hfs} are listed in Table I. The CPT resonance can be excited by bichromatic light fields, ω_1 and ω_2.

^{85}Rb and ^{87}Rb vapors have the same wavelengths for D1 and D2 lines, but their f_{hfs} values are different. The f_{hfs} for ^{85}Rb is 3.0 GHz [21], which is less than one-half that of ^{87}Rb and one-third that of Cs. Using ^{85}Rb vapor decreases f_{hfs} generated from a local oscillator to excite the CPT resonance. The CPT resonances of ^{85}Rb and ^{87}Rb can be observed in a natural Rb gas cell because a natural mixture of Rb isotopes consists of both ^{85}Rb and ^{87}Rb atoms.

III. EXPERIMENTAL CONFIGURATION

A schematic of the CPT atomic clock test system is shown in Fig. 2. The Rb gas cell with 3 cm length consists of a natural mixture of Rb atoms and 1.5 kPa of N_2 buffer gas, and its temperature was controlled at 38 ºC to stabilize the CPT resonant frequency. To improve the long-term stability, the cell was placed inside a double magnetic shield together with a solenoid to prevent environmental magnetic fluctuations. A small homogeneous magnetic field of 4.5-μT flux density parallel to the optical axis was generated around the vapor cell. To excite Rb at the D1 and D2 lines between the ground state, $5^2S_{1/2}$, and the excited state, $5^2P_{2/1}$ and $5^2P_{2/3}$, single-mode vertical-cavity surface-emitting lasers (VCSELs) with 780- and 795-nm wavelengths were used, respectively. In both cases, each VCSEL was driven by a 1-mA dc injection current using a bias-T and was modulated by an RF source to generate first order sidebands around the laser carrier. The RF modulation frequency was set at 1.5, 3.0, 3.4, and 6.8 GHz, which were both at the full- and half-ground-state hyperfine frequencies of ^{85}Rb and ^{87}Rb. For the 1.5- and 3.4-GHz modulation frequency, two first order sidebands were used to excite from two ground states, $|g_1\rangle$ and $|g_2\rangle$, to the excited state, $|e\rangle$. For the 3.0- and 6.8-GHz modulation frequency, the carrier and a first order sideband were used. The linearly polarized optical output from the VCSEL was sent through a quarter wave plate to create a circular polarization and was attenuated by natural-density (ND) filters. At the entrance of the vapor cell, a 20-μW/cm^2 σ^+ circular-polarized light beam of 4 mm in diameter was remained. The laser temperature was controlled to maintain the absorption maximum point of the two hyperfine structures F = 1 and F = 2 for ^{87}Rb, F = 2 and F = 3 for ^{85}Rb. A photodiode detected the intensity transmitted through the cell

IV. ABSORPTION PROFILES OF Rb D1 LINE

The absorption profiles were scanned around the Rb D1 line as shown in Fig. 3. In the figure, both ^{85}Rb and ^{87}Rb profiles are overlapped by reason of the natural mixture of Rb isotopes. The isotope ratio of ^{85}Rb/^{87}Rb is 2.6, therefore, the absorptions of ^{85}Rb were larger than that of ^{87}Rb. The frequency was normalized by the F = 3 absorption frequency of ^{85}Rb. With RF modulation applied, the absorption profiles changed significantly because of the generated laser side-bands. In the experiments, the input RF power was optimized as the amplitudes of the CPT resonances were maximized.

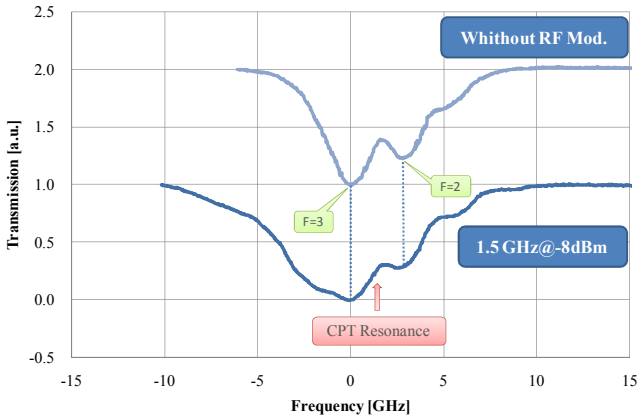

Figure 3. Absorption profile for Rb D1 line with 1.5 GHz modulation

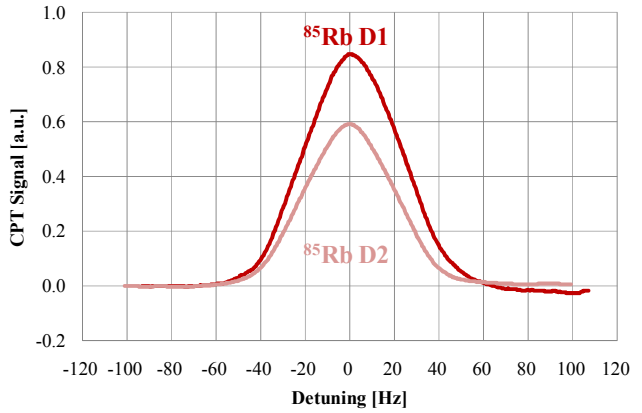

Figure 4. Line shapes of ^{85}Rb CPT resonances; center frequencies was 1.517 867 814 GHz and 1.517 867 855 GHz for D1 and D2 lines respectively.

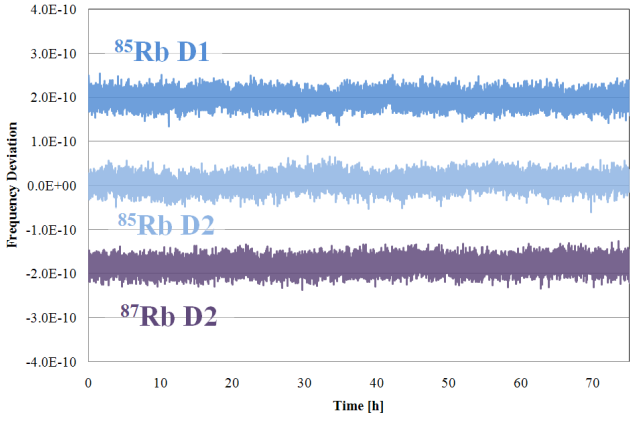

Figure 5. Frequency deviations of Rb D1 and D2 CPT Clocks

For the RF modulation of ^{87}Rb atoms (3.0- and 6.8-GHz modulation), the CPT resonances were observed; however, the resonance amplitudes were too weak to measure the frequency stabilities because the laser light was used for the excitation of ^{85}Rb atoms. Therefore, only ^{85}Rb D1-line characteristic was observed in the experiment. Figure 4 shows an example of the CPT resonances for ^{85}Rb obtained through simple numerical integration of the lock-in amplifier in-phase signal [18]. The CPT amplitude of D1 line is 1.5 times higher than that of D2 line because of different excited-state hyperfine structure between the two excitation lines [21]. The CPT resonance frequency was shifted upward 1.6 kHz as a result of buffer gas collisions and light shift. The full-width at half maximum was ~50 Hz (Q value of 3.0×10^7) for ^{85}Rb and ~120 Hz (Q value of 5.7×10^7) for ^{87}Rb with 1.5- and 6.8-GHz RF modulation, respectively.

V. Frequency Deviation of Rb CPT Clocks

The frequency stability was measured using the CPT-clock test system as shown in Fig. 2. A 10-MHz oven-controlled crystal oscillator (OCXO) was connected to an RF signal generator as a reference source for controlling the RF modulation frequency. A lock-in at 100 kHz was used to lock the laser to the Rb absorption maximums with controlling laser temperature, and a lock-in at 125 Hz kept the RF frequency at the CPT resonance frequency by controlling the OCXO output frequency. The frequency counter was locked using the Cs standard, and the OCXO output frequency was measured every 2 seconds. Figure 5 shows the frequency deviation of the Rb CPT clock. In the case of D2 excitation, the clock were operated at a 6.8-GHz (+3.0 dBm) modulation for ^{87}Rb and 1.5-GHz (-2.6 dBm) for ^{85}Rb. Their stabilities were improved from the previous results in [19] by developing the VCSEL temperature control system and the magnetic shields of the gas cell. In the case of D1 excitation, the clock were operated at a 1.5-GHz (-8.0 dBm) modulation for ^{85}Rb. The values were normalized using the initial frequencies, and 2×10^{-10} was added to the values of ^{85}Rb D1 and subtracted from the values of ^{87}Rb D2 for clear observation. The curves of ^{85}Rb show more fluctuations than that of ^{87}Rb. The frequency fluctuations could have been affected by these sensitivity differences even though the gas-cell and laser temperatures were controlled. Since the ground-state hyperfine frequency for ^{85}Rb was nearly half that for ^{87}Rb, its Q factor was also nearly half that for ^{87}Rb. Therefore, the frequency shifts caused by temperature fluctuations, laser power fluctuations, magnetic field fluctuations, RF modulation fluctuations, etc. were roughly twice as sensitive as those for ^{87}Rb.

Allan deviations estimated from the data (Fig.5) are shown in Fig. 6. Since the time constant of the RF signal generator connected to the OCXO was few hundred milliseconds, the time constant of the second feedback loop was set to 2 seconds. Therefore, the short-term stability in the range of τ = 2 to 100 was dominant for the short-term stability of the OCXO itself, and all curves were ~$2\times10^{-11}/\tau^{1/2}$. In the region

of $\tau > 100$, the minimum values was 2.3×10^{-12} at $\tau = 2.6\times10^{2}$ for ^{85}Rb D2, 1.3×10^{-12} at $\tau = 6.6\times10^{4}$ for ^{85}Rb D1, and 1.3×10^{-12} at $\tau = 3.3\times10^{4}$ for ^{87}Rb D2 line. The long-term stabilities was $< 2.5\times10^{-12}$/day for ^{85}Rb D1, $< 4.0\times10^{-12}$/day for ^{85}Rb D2, and $< 3.5\times10^{-12}$/day for ^{87}Rb D2-line. Using the CPT resonances of Rb atoms improved the long-term stabilities 25 times better than that of OCXO (10^{-10}). In addition, the frequency stability of ^{85}Rb D1 line is better than that of ^{85}Rb D2 line in the region of $\tau > 2000$. These results indicate that the ^{85}Rb CPT atomic clock is able to keep demanded long-term stability $\sim10^{-11}$/day, and that using ^{85}Rb atoms is suitable for low-power operation.

VI. CONCLUSIONS

An ^{85}Rb D1-line CPT atomic clock was investigated. Experiments show that the frequency deviations for ^{85}Rb D1- and D2-lines can be measured using a same experimental setup except for VCSEL wavelength and RF power. The long-term stabilities were $< 2.5\times10^{-12}$/day for ^{85}Rb D1-line and $< 4.0\times10^{-12}$/day for D2-line. In the case of D1-line, the RF frequency was 1.5 GHz and its power was only -8.0 dBm. In addition, the long-term stability of ^{85}Rb D1 line was better than that of ^{85}Rb D2 line. These results indicate that the ^{85}Rb D1-line CPT atomic clock has good long-term stability and consumes less than half the RF power as a ^{87}Rb one.

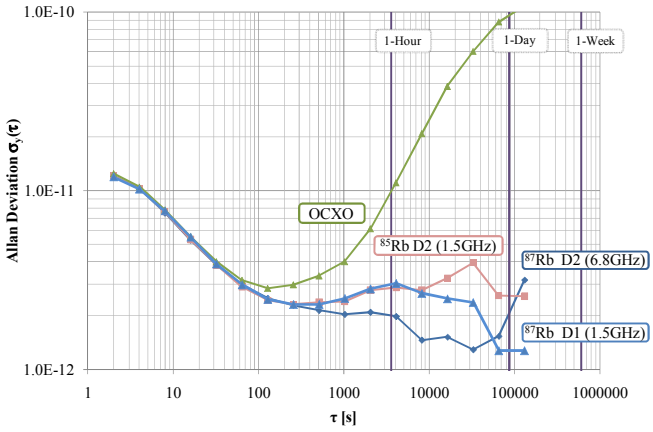

Figure 6. Allan deviations of ^{85}Rb and ^{87}Rb CPT atomic

REFERENCES

[1] F. G. Major, *The quantum beat: Principles and Applications of Atomic Clocks*, (Springer, 1998)

[2] J. Vig: "Military applications of high accuracy frequency standards and clocks," IEEE Trans. Ultrason. Ferroelec. Freq. Cont. **40,** 1993, pp. 522-527.

[3] S. Knappe, R. Wynands, J. Kitching, H.G. Robinson, and L. Hollberg, "Characterization of coherent population-trapping resonances as atomic frequency references," J. Opt. Soc. Am. B., **18**, 2001, pp. 1545-1553.

[4] J. Kitching, S. Knappe, N. Vukicevic, L. Hollberg, R. Wynands, and W. Weidemann, "A microwave frequency reference based on VCSEL-driven dark line resonances in Cs vapor," IEEE Trans. Instrum. Meas., **49**, 2000, pp. 1313-1317.

[5] J. Kitching, H.G. Robinson, L. Hollberg, S. Knappe, and R. Wynands, "Optical-pumping noise in laser-pumped, all-optical microwave frequency references," J. Opt. Soc. Am. B., **18**, 2001, pp. 1676-1683.

[6] R. Lutwak, D. Emmons, W. Riley, and R. M. Garvey, "The chip-scale atomic clock – Coherent population trapping vs. Conventional interrogation", Proceedings of the 34th Annual Precise Time and Time Interval (PTTI) Systems and Applications Meeting, 2002, pp. 539-550.

[7] L. Liew, S. Knappe, J. Moreland, H. Robinson, L. Hollberg and J. Kitching, "Microfabricated alkali atom vapor cells," Appl. Phys. Lett., **84**, 2003, pp. 2694-2696.

[8] R. Lutwak, D. Emmons, T. English, W. Riley, "The chip-scale atomic clock – Recent development progress", Proceedings of the 35th Annual Precise Time and Time Interval (PTTI) Systems and Applications Meeting, San Diego, CA, 2003, pp. 467-478.

[9] S. Knappe, L. Liew, V. Shah, P. Schwindt, J. Moreland, L. Hollberg and J. Kitching, "A microfabricated atomic clock," Appl. Phys. Lett., **85**, 2004, pp. 1460-1462.

[10] R. Lutwak, J. Deng, W. Riley, M. Varghese, J. Leblanc, G. Tepolt, M. Mescher, D. K. Serkland, K. M. Geib, and G. M. Peake: "The chip-scale atomic clock - Low-power physics package", Proceedings of the 36th Annual Precise Time and Time Interval (PTTI) Systems and Applications Meeting, 2004, pp. 339-354.

[11] S. Knappe, P. Schwindt, V. Shah, L. Hollberg, J. Kitching, L. Liew, and J. Moreland, "A chip-scale atomic clock based on ^{87}Rb with improved frequency stability," Opt. Exp., **13**, 2005, pp. 1249-1253.

[12] S. Knappe, V. Gerginov, P. D. D. Schwindt, V. Shah, H. G. Robinson, L. Hollberg, and J. Kitching, "Atomic vapor cells for chip-scale atomic clocks with improved long-term frequency stability," Opt. Lett., **30**, 2005, pp. 2351-2353.

[13] V. Gerginov, S. Knappe, V. Shah, P. D. D. Schwindt, L. Hollberg, and J. Kitching, "Long-term frequency instability of atomic frequency references based on coherent population trapping and microfabricated vapor cells," J. Opt. Soc. Am. B, **23**, 2006, pp. 593-597.

[14] R. Wynands, A. Nagel, "Precision spectroscopy with coherent dark states", Appl. Phys. B **68**, 1999, pp. 1-25.

[15] J. Vanier, "Atomic clocks based on coherent population trapping: a review", Appl. Phys B, **81**,2005, pp. 421-442

[16] A. S. Sedra: *Microelectronic Circuits* (Oxford, New York) 5th ed., Chap. 4, 2004, pp. 345.

[17] R. Lutwak, P. Vlitas, M. Varghese, and M. Mescher: "The MAC – A Miniature Atomic Clock," Proc. Int. Freq. Cont. Symp., 2005, pp. 752-757.

[18] M. Merimaa, T. Lindvall, I. Tittonen, and E. Ikonen: "All-optical atomic clock based on coherent population trapping in ^{85}Rb," J. Opt. Soc. Am. B **20**, Issue 2, 2003, pp. 273-279.

[19] S. Goka, T. Okura, M. Moroyama, and Y. Watanabe, "Low Power ^{85}Rb CPT Atomic Clock", Proc. Int. Freq. Cont. Symp., 2008, pp. 103-106.

[20] S. Goka: "Experimental Study of Low Power ^{85}Rb CPT Atomic Clock", Proc. 2nd Int. Work. Piezo-devices Based on Latest MEMS Tech., 2008.

[21] M Stähler, R. Wynands, S. Knappe, J. Kitching, L. Hollberg, A. Taichenachev, and V. Yudin, "Coherent population trapping resonances in thermal ^{85}Rb vapor: D_1 vs D_2 line excitation," Optics Letters, **27**, 2002, pp. 1472-1474.